

## Resonant-Solar-Neutrino-Oscillation Experiments

Stephen J. Parke and Terry P. Walker

*Fermi National Accelerator Laboratory, Batavia, Illinois 60510*

(Received 28 July 1986)

The results of a detailed calculation of the effects of resonant neutrino oscillations in the sun on the current and proposed solar-neutrino experiments are presented. Analytic results are used for the electron-neutrino survival probability so that a sophisticated model for both the production distribution of the solar neutrino sources and the solar electron-number density can be employed. Contour plots for the electron-neutrino capture rate, in the plane of the mass difference squared versus vacuum mixing angle, are given for the current  $^{37}\text{Cl}$  experiment and the proposed  $^{71}\text{Ga}$  detector.

PACS numbers: 96.60.Kx

Recently, Mikheyev and Smirnov<sup>1</sup> have shown that the matter neutrino oscillations of Wolfenstein<sup>2</sup> can undergo resonant amplification in the solar interior thereby reducing the flux of electron neutrinos emerging from the sun. This mechanism may be the solution of the solar-neutrino puzzle.<sup>3,4</sup> Subsequently, Bethe and others<sup>5,6</sup> have refined and restated the idea of Mikheyev and Smirnov, pointing out that there are three general regions of parameter space in which the solar electron-neutrino flux is sufficiently reduced. Unfortunately, all of these papers either use a crude solar model or do not consider the nonadiabatic region of parameter space.

In this Letter we correct this deficiency and present contour plots of electron-neutrino capture rates in the plane of the mass difference squared versus vacuum mixing angle, for both the chlorine experiment and the pro-

posed gallium detector. These plots are the results of detailed calculations of the solar-electron-neutrino capture rates in  $^{37}\text{Cl}$  and  $^{71}\text{Ga}$  as a function of mass difference squared and vacuum mixing angle. We use an analytic form for the neutrino transformation probability which is valid in both the adiabatic and nonadiabatic regimes,<sup>7</sup> in conjunction with a relatively sophisticated solar model.

If neutrinos are massive, then the flavor and mass eigenstates are not necessarily identical; however, a general neutrino state can always be written in the flavor basis,<sup>8</sup>

$$| \nu(t) \rangle = c_e(t) | \nu_e \rangle + c_\mu(t) | \nu_\mu \rangle. \quad (1)$$

In the ultrarelativistic limit, the evolution of this general neutrino state, in matter, is described by the following Schrödinger-type equation,<sup>2</sup>

$$i \frac{d}{dt} \begin{pmatrix} c_e \\ c_\mu \end{pmatrix} = \frac{1}{2} \begin{pmatrix} -\Delta_0 \cos(2\theta_0) + \sqrt{2} G_F N_e & \Delta_0 \sin(2\theta_0) \\ \Delta_0 \sin(2\theta_0) & \Delta_0 \cos(2\theta_0) - \sqrt{2} G_F N_e \end{pmatrix} \begin{pmatrix} c_e \\ c_\mu \end{pmatrix}, \quad (2)$$

where  $\Delta_0 \equiv \delta m^2/2k = (m_2^2 - m_1^2)/2k$ ,  $m_i$  are the neutrino masses,  $k$  is the neutrino energy,  $\theta_0$  is the vacuum mixing angle,  $G_F$  is the Fermi constant, and  $N_e$  is the electron-number density. The matter mass eigenstates, in an electron density  $N_e$ , are

$$\begin{aligned} | \nu_1 \rangle &= \cos\theta_N | \nu_e \rangle - \sin\theta_N | \nu_\mu \rangle, \\ | \nu_2 \rangle &= \sin\theta_N | \nu_e \rangle + \cos\theta_N | \nu_\mu \rangle, \end{aligned} \quad (3)$$

where the matter mixing angle  $\theta_N$  is given by  $\sin(2\theta_N) = \Delta_0 \sin(2\theta_0)/\Delta_N$ , with

$$\Delta_N = \{ [\Delta_0 \cos(2\theta_0) - \sqrt{2} G_F N_e]^2 + \Delta_0^2 \sin^2(2\theta_0) \}^{1/2}.$$

At resonance the electron density is  $N_e^{\text{res}} = \Delta_0 \cos(2\theta_0)/\sqrt{2} G_F$ , and the matter mixing angle  $\theta_N^{\text{res}} = \pi/4$ . Above resonance,  $\theta_N$  satisfies  $\pi/4 < \theta_N < \pi/2$ .

We use the approximation that the electron density in the Sun varies linearly in the region where transitions between the matter-mass eigenstates are important. Then the probability of detecting an electron neutrino, averaged over the production and the detection positions, is

given by<sup>7</sup>

$$\bar{P}_{\nu_e} = \frac{1}{2} + \left( \frac{1}{2} - P_x \right) \cos(2\theta_0) \cos(2\theta_N), \quad (4)$$

where  $P_x$  is the Landau-Zener probability for transitions between the matter mass eigenstates during single resonance crossing:

$$P_x = \exp \left[ - \frac{\pi}{2} \frac{\sin^2(2\theta_0)}{2 \cos(2\theta_0)} \frac{\delta m^2/2k}{| \mathbf{n} \cdot \nabla \ln N_e |_{\text{res}}} \right]. \quad (5)$$

The unit vector  $\mathbf{n}$  is in the direction of propagation of the neutrino. For nonresonance crossing,  $P_x = 0$ , and for double-resonance crossing,  $P_x$  in Eq. (4) should be replaced by  $2P_x(1 - P_x)$ . From Eqs. (4) and (5) one can see that the electron-neutrino detection probability depends only on the electron density in the solar interior at production and the logarithmic slope of this density at resonance crossing. In Fig. 1(a) we give the fit for  $N_e(r) = \rho(r) Y_e(r)/m_N$  used in our calculations, which was obtained from the solar model of Bahcall *et al.*<sup>9</sup>

The solar-electron-neutrino capture rate for a detector

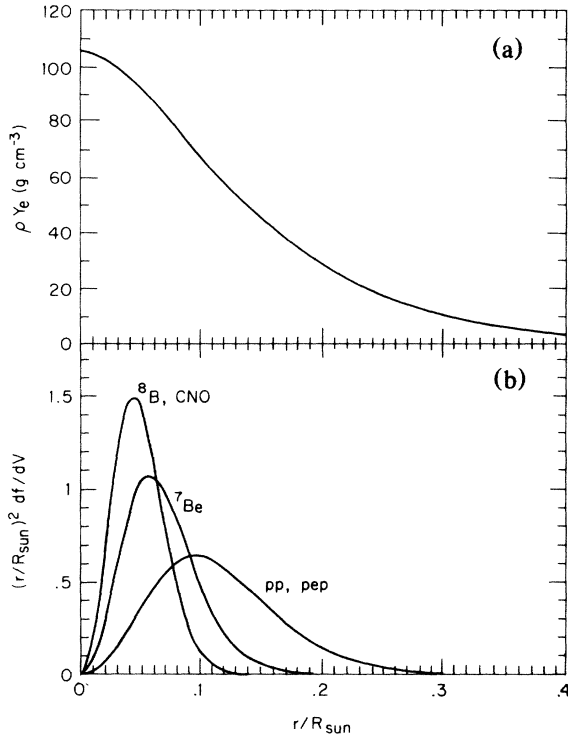


FIG. 1. Fits to the solar model of Bahcall: (a)  $\rho Y_e = m_N N_e$  and (b)  $(r/R_{\text{sun}})^2$  times the fractional neutrino volume emissivity for the indicated processes, both as functions of fractional solar radius.

characterized by an electron-neutrino capture cross section  $\sigma(E)$  and energy threshold  $E_0$  is

$$\sum_{\text{processes}} \int_{E_0}^{\infty} (d\Phi_{\nu}/dE) \sigma(E) dE. \quad (6)$$

The sum is taken over all neutrino sources in the Sun and  $d\Phi_{\nu}/dE$  is the differential electron-neutrino flux of a given source at the Earth's surface. To include the reduction in the electron-neutrino flux from the Sun due to resonant neutrino oscillations, the differential electron-neutrino flux for each process was calculated as

$$d\Phi_{\nu}/dE \propto W(E) \int_{\text{sun}} dV \bar{P}_{\nu_e} df/dV, \quad (7)$$

where  $W(E)$  is the standard weak-interaction energy distribution for the neutrinos of a given process and  $df/dV$  is the fraction of the standard-solar-model flux coming from a given solar volume element for this process. In Fig. 1(b) we have plotted  $r^2 df/dV$  for the various processes, which were calculated from the solar model of Bahcall *et al.* Note that we have assumed that the spatial distributions for *pep* and CNO neutrinos are given by those for *pp* and  $^8\text{B}$  neutrinos, respectively.<sup>10</sup> We normalize  $d\Phi_{\nu}/dE$  for each process by demanding that the energy and solar-volume integrations of Eq. (6) yield the capture rates quoted by Bahcall *et al.* when  $\bar{P}_{\nu_e} = 1$ .

The cross sections  $\sigma(E)$  used for the  $^{37}\text{Cl}$  and  $^{71}\text{Ga}$

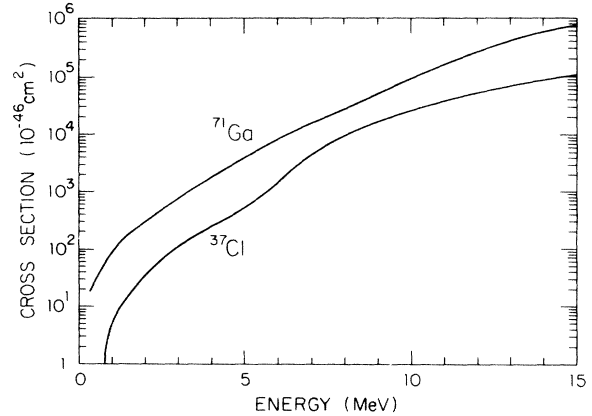


FIG. 2. Neutrino-capture cross sections as a function of energy for both  $^{37}\text{Cl}$  and  $^{71}\text{Ga}$ .

detectors, whose thresholds are 814 and 236 keV, respectively, are given in Fig. 2. The  $^{37}\text{Cl}$  cross section is derived from the data of Bahcall *et al.*<sup>9</sup> and the  $^{71}\text{Ga}$  cross section is a fit to the low-energy calculation of Bahcall<sup>11</sup> and the higher-energy calculations of Grotz, Klappdor, and Metzinger.<sup>12</sup> In Table I we list two sets of expected capture rates for both the chlorine and gallium experiments and the maximum neutrino energy for each solar neutrino source. Model A is taken from the values of Bahcall *et al.*<sup>4</sup> and model B, reported by Bahcall,<sup>13</sup> reflects recent changes in the expected solar-neutrino capture rate. The most important change is in the estimation of the Sun's opacity, which alters the solar temperature profile. A comparison between these two models demonstrates the insensitivity of the allowed region of parameter space to small changes in the solar model. The value of 16 solar neutrino units (SNU) for the  $^8\text{B}$  rate in model A for the gallium experiment is an average of the new predictions of Grotz, Klappdor, and Metzinger<sup>12</sup> and Mathews *et al.*<sup>14</sup>

In Figs. 3 and 4, we present electron-neutrino capture-rate contours (iso-SNU contours) for the  $^{37}\text{Cl}$  and  $^{71}\text{Ga}$  experiments as a function of  $\delta m^2$  and  $\sin^2(2\theta_0)/\cos(2\theta_0)$

TABLE I. Neutrino sources and capture rates for two solar models.

Process	$E_{\nu}^{\text{max}}$ (MeV)	Chlorine (SNU)		Gallium (SNU)	
		Model A	Model B	Model A	Model B
$^8\text{B}$	14.06	4.3	5.75	16.0	18.0
$^7\text{Be}$	0.861 (90%) +0.383 (10%)	1.0	1.1	27	34
<i>pp</i>	0.420	0	0	70	70
<i>pep</i>	1.44	0.23	0.20	2.5	3.0
$^{13}\text{N}$	1.199	0.08	0.10	2.6	4.0
$^{15}\text{O}$	1.732	0.26	0.35	3.5	6.0
Total		5.9	7.5	122	135

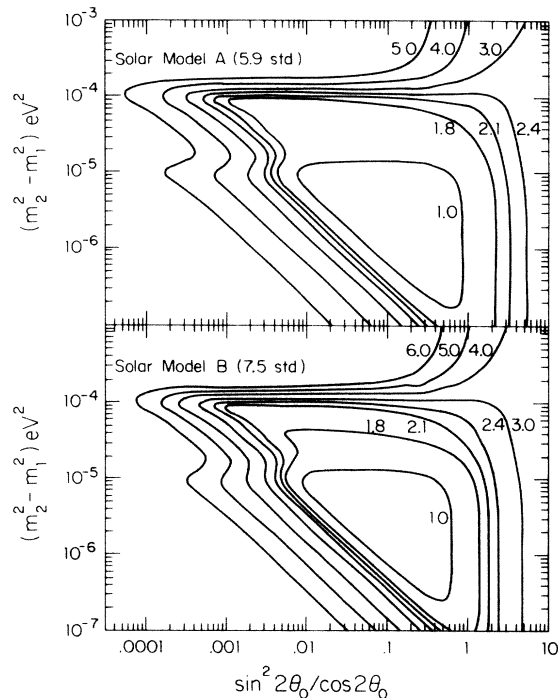


FIG. 3. Iso-SNU contours for the  $^{37}\text{Cl}$  experiment for the solar models listed in Table I. The contours are labeled with their corresponding SNU values.

for the two solar models discussed earlier. The  $1\sigma$  deviations from the Davis, Harmer, and Hoffman<sup>3</sup> result of 2.1 SNU are the 2.4- and 1.8-iso-SNU contour lines in Fig. 3. The similarity of the shape of these plots for the two solar models reflects the insensitivity of the resonant oscillation process to small changes in the structure of the Sun. However, the position of individual contours does change, because of changes in the contributions from the individual neutrino sources. The generic structure of these total-SNU plots is due to the superposition of triangular iso-SNU contours associated with each individual neutrino source contributing to a given total SNU value. These individual contours owe their shape to the appropriate isoprobability contour<sup>7</sup> and their position is determined by the typical energy scale and production electron density of the individual neutrino source. For each neutrino source the resonance mechanism becomes important, provided that  $\theta_0 > 0.01$ , as soon as  $\delta m^2$  becomes small enough so that the average resonant electron density for that source is less than the solar electron density at the production site. This occurs when  $\delta m^2$  is approximately equal to  $1.5 \times 10^{-4}$ ,  $1.2 \times 10^{-5}$ , and  $3.7 \times 10^{-6}$  eV<sup>2</sup> for the  $^8\text{B}$ ,  $^7\text{Be}$ , and  $pp$  neutrinos, respectively. Below these values the individual neutrino sources have contours which are diagonals of slope minus one coming from the form of the transition probability between adiabatic states, Eq. (5). The intersection of these diagonal lines with the turning on of resonance for  $^8\text{B}$ ,  $^7\text{Be}$ , and  $pp$  is responsible for the shoulders at small

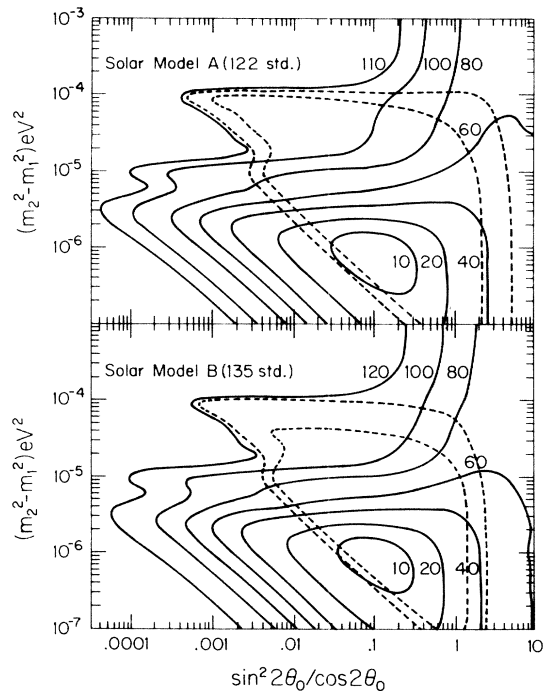


FIG. 4. Iso-SNU contours for a  $^{71}\text{Ga}$  detector for the solar models listed in Table I.  $1\sigma$  deviations from the Davis  $^{37}\text{Cl}$  experimental result are shown by the dashed contours. The solid curves are labeled with their appropriate  $^{71}\text{Ga}$  SNU values.

$\sin^2(2\theta_0)/\cos(2\theta_0)$  in the contour plots. The vertical sections of the contours, at large  $\theta_0$ , occurs because for large  $\theta_0$  both adiabatic states have a large component of electron neutrino.

From Fig. 4 we see that the results of the  $^{71}\text{Ga}$  experiment can range from 10 to 120 SNU and still be compatible with the  $^{37}\text{Cl}$  experiment. In general, a given gallium contour crosses the  $2.1 \pm 0.3$  chlorine contour at least twice, and therefore the results of the  $^{71}\text{Ga}$  experiment will leave a twofold degeneracy in  $(\delta m^2, \theta_0)$  space. If one accepts the theoretical prejudice against large vacuum angles provided by seesaw models<sup>15</sup> this degeneracy is removed. Unfortunately, the degeneracy is continuous for that region of parameter space corresponding to a  $^{37}\text{Cl}$  rate of  $2.1 \pm 0.3$  SNU and a  $^{71}\text{Ga}$  rate greater than 100 SNU. In this region *only* the  $^8\text{B}$  neutrinos are affected by the resonance phenomena. Also, in this region of parameter space the two experiments will not be able to distinguish between a small temperature change at the solar core and the resonant-neutrino-oscillation mechanism. This is due to the relatively strong temperature dependence of the  $^8\text{B}$  neutrino flux.<sup>16</sup> It is only when the  $^{71}\text{Ga}$  SNU rate is depleted below that of merely removing the  $^8\text{B}$  component (i.e., appreciably less than 110 SNU), so that reduction of the less temperature-sensitive neutrinos ( $^7\text{Be}$  and  $pp$ ) becomes necessary, that the resonant oscillation mechanism becomes a likely solution to the solar-neutrino problem.

We would like to thank Rocky Kolb for many helpful

discussions and for making us aware of John Bahcall's new results, and John Bahcall for discussing the changes which give rise to his new model.

---

<sup>1</sup>S. P. Mikheyev and A. Yu. Smirnov, in Proceedings of the Tenth International Workshop on Weak Interactions and Neutrinos, Savonlinna, Finland, 1985 (to be published), and *Nuovo Cimento* **9C**, 17 (1986).

<sup>2</sup>L. Wolfenstein, *Phys. Rev. D* **17**, 2369 (1978), and **20**, 2634 (1979).

<sup>3</sup>R. Davis, D. S. Harmer, and K. C. Hoffman, *Phys. Rev. Lett.* **20**, 1205 (1968).

<sup>4</sup>J. N. Bahcall, B. T. Cleveland, R. Davis, and J. K. Rowley, *Astrophys. J.* **292**, L79 (1985).

<sup>5</sup>H. A. Bethe, *Phys. Rev. Lett.* **56**, 1305 (1986).

<sup>6</sup>A. Messiah, S. P. Rosen, and M. Spiro, in Proceedings of the Twenty-First Rencontre de Moriond Workshop on Massive Neutrinos in Physics and Astrophysics, Tignes, France, January 1986 (to be published); S. P. Rosen and J. M. Gelb, *Phys. Rev. D* **34**, 969 (1986); E. W. Kolb, M. S. Turner, and T. P. Walker, *Phys. Lett.* **175B**, 478 (1986); V. Barger, R. J. N. Phillips, and K. Whisnant, *Phys. Rev. D* **34**, 980 (1986); J. Bouchez, M. Cribier, J. Rich, M. Spiro, D. Vignard, and W. Hampel, Département de Physique des Particules Élémentaires, Centre d'Etudes Nucléaires de Saclay Report No. 86-10, 1986 (to be published).

<sup>7</sup>S. Parke, *Phys. Rev. Lett.* **57**, 1275 (1986).

<sup>8</sup>The other flavor eigenstate could just as well be  $\nu_e$ .

<sup>9</sup>J. N. Bahcall, W. F. Huebner, S. H. Lubow, P. D. Parker, and R. K. Ulrich, *Rev. Mod. Phys.* **54**, 767 (1982).

<sup>10</sup>The CNO distributions are undoubtedly tighter than  $^8\text{B}$  because of their more-sensitive dependence on temperature, but the inaccuracy introduced by this approximation is negligible.

<sup>11</sup>J. N. Bahcall, in Proceedings of the Neutrino Mass Mini-conference, Telemark, Wisconsin, 1980, edited by V. Barger and D. Cline (unpublished).

<sup>12</sup>K. Grotz, H. V. Klapdor, and J. Metzinger, *Astron. Astrophys.* **154**, L1 (1986).

<sup>13</sup>J. N. Bahcall, in Proceedings of the International Symposium on Weak and Electromagnetic Interactions in Nuclei, Heidelberg, 1-5 July 1986 (to be published).

<sup>14</sup>G. J. Mathews, S. D. Bloom, G. M. Fuller, and J. N. Bahcall, *Phys. Rev. C* **32**, 796 (1985).

<sup>15</sup>T. Yanagida, *Prog. Theor. Phys.* **B135**, 66 (1978); M. Gell-Mann, P. Ramond, and R. Slansky, in *Supergravity*, edited by P. van Nieuwenhuizen and D. Freedman (North-Holland, Amsterdam, 1979).

<sup>16</sup>In the case where a  $^{71}\text{Ga}$  rate of  $\geq 100$  SNU is measured, a measurement of the  $^8\text{B}$  solar-neutrino spectrum (see Rosen and Gelb, Ref. 6) or the flavor-independent solar-neutrino flux [see S. Weinberg, in Proceedings of the Twenty-Third International Conference on High Energy Physics, Berkeley, 16-23 July 1986 (to be published)] would allow us to distinguish between changes in the solar model and resonant neutrino oscillations.